Monte Carlo Simulation of Grain Growth Behavior in ZnO Thin Film during Crystallization Process

Leila Challat [1]
Azzedine Bellel [1]
Salah Sahli [2]

[1] Laboratoire d'Etude des Matériaux Electronique pour Applications Médicales (LEMEAMED), Faculté des Sciences de la Technologie, Université Frères Mentouri Constantine1, Constantine 25000, ALGERIA
[2] Laboratoire de Microsystèmes et Instrumentation (LMI), Faculté des Sciences de la Technologie, Université Frères Mentouri Constantine1, Constantine 25000, ALGERIA

In this work, a theoretical model for the prediction of the grain growth behavior in zinc oxide (ZnO) thin film during the crystallization step has been developed. The model based on the Population Balance Equations (PBE) that includes nucleation and grain growth has been used in case of 150 nm thick ZnO layer elaborated by sol gel method on silicon substrate. Monte Carlo (MC) simulation has been used for resolving the population balance to predict annealing temperature effect on grain growth behavior. The results showed that the distribution of thin film grain sizes follows a Gaussian law with temperature, which predicts an increase of the grain size from 20 to 24 nm with increasing annealing temperature from 350°C to 500°C. The growth of larger grain with the preferential orientation and crystallinity percentage equal to 46. 59% has been obtained at annealing temperature of 500°C. Numerical results have been correlated to the structural and morphological analysis carried out by x-ray diffraction (XRD) and atomic force microscopy (AFM), respectively.

***Keywords*:** Sol-gel method; Thin films; Zinc oxide; Grain growth
Received: 10 October 2024; **Revised:** 04 January; **Accepted:** 11 January 2025

1. Introduction

In recent years, with the development of technology, Zinc oxide (ZnO) becomes the most promising material for use in various applications due to their many advantageous characteristics. Firstly, ZnO is a II-VI semiconductor with wide band gap (~3.37eV) corresponding to ultraviolet range with higher energy than of visible light. The high excitation binding energy (~60 meV) allows their use as a blue or ultraviolet laser material [1]. Moreover, ZnO is much abundant and nontoxic to environment [2]. Secondly, ZnO properties such as morphology, crystalline structure, orientation and concentration can be precisely controlled by the deposition technique and process parameters to improve their electrical and optical properties. In fact, ZnO crystallizes in the well know hexagonal wurtzite phase as a stable crystal structure at ambient temperature and pressure [3]. ZnO can grow in three directions, which leads to the diversity of its structure such as: nanoparticle, nanorod, microspheres, nanowire and nanosheet, depending on the deposition parameters and technique [4]. The recent development and research aim to synthesize ZnO thin film with grain growth according to the specific crystallographic direction [002] called the preferential orientation [5]. Chemical deposition of thin films from an aqueous solution represents an alternative approach to produce high-quality ZnO thin film due to its simplicity and low cost. In fact, several chemical deposition methods have been used for the elaboration of thin films such-as: spray pyrolysis [6], electro-deposition process [7] and sol gel [8]. Among all these methods, sol gel has many advantages in producing thin films, such as: lower crystallization temperature, homogeneous composition [9] and requiring low cost equipment [10]. The quality of ZnO thin film synthesized by sol gel method can be affected by the experimental conditions like: solution concentration [11], aging time [12], nature of substrate [13], annealing temperature [14] and time of annealing [15]. The thermal annealing is generally used in thin film semiconductors to improve the crystalline quality, grain growth and optoelectronic proprieties. Usually, the heat treatment process leads to the formation of larger grains, decreasing surface roughness and improving device performance. Several research groups have reported the effect of annealing conditions on the structural properties of ZnO thin films. M. Arif et al [16] investigated the effect of annealing temperature (300, 400 and 500°C) on structural and optical properties of ZnO thin films elaborated by sol gel method. They have showed that the increase in annealing temperature induced a decrease in the full width at half-maximum (FWHM), leading to the increase of the crystallite size from 13 to 23 nm and the decrease of the optical band gap from 3.14 to 3.02 eV. Using the same annealing conditions, similar observations was reported by B. Sharmila et al [17] and L. Arab et al [18]. In all such studies, authors showed that the average crystallite size continuously increases with increasing annealing temperature. Therefore, it is important to control grain growth in oxide thin film in order to manipulate structural proprieties such as grain size and orientation which directly determine electrical and optical proprieties. Generally, thin films prepared by chemical solution deposition (CSD) methods are

obtained in the crystallization step by post deposition thermal annealing. This step allows the grains growth in thin film and changes crystal orientation [19]. Grain growth which refers to the increase in grain size at high temperature enables larger grains to grow in such a manner that consuming smaller grains due to the movement of grain boundaries .This reduces the total Gibbs free energy of the microstructure and decrease the total grain number but increase the average grain size [20].

In the last few years, considerable attention has been paid to the development of different theoretical models for the simulation of the grain growth. Numerical simulation methods present a powerful tool for designing and predicting the film properties. These methods provide a first rapid evaluation of the film microstructure and can give an overview of the parameters involved, while reducing the development and optimization costs. Among the most developed simulation method, we found phase-field [21] and the Monte Carlo Potts models [22]. Although the reported models are based on different ideas describing the grain growth in polycrystalline microstructure, they reach generally similar conclusions that the grain growth obeys to the parabolic law with normal or abnormal grain size distribution. In this context, there are two types of grain growth in thin film. The first type is the normal grain growth which describes the average grain size variation with a parabolic growth law. The grain size distribution follow a log-normal law over time in which the smaller grain are more existed compared with lager grains. The growth in this case is driven by the minimization of total free energy of films. The second type is abnormal growth which is characterized by the non Gaussian distribution of grain size with time and the formation of large grains expense of smaller one [23]. V. Kumar et al [24] have studied the effect of annealing on structural properties of ZnO thin films prepared by sol gel method. They found that the grain size distribution obeys to the log-normal distribution by fitting the measured distribution at each annealing time. Most of the previous researches on grain growth in thin films are limited on polycrystalline grain structure.

The aim of this work is to study the ZnO grain growth during crystallization step. In fact, the crystallization is associated with the transformation of the thin film from its amorphous state to a crystalline state. This transformation is governed by two physical processes; nucleation and growth which define the film microstructure [25]. To the best of our knowledge, the grain growth mechanism during ZnO thin film crystallization has been studied only by N. Bouhssira et al [26] and O.A. Hammadi [27]. The authors demonstrated that the parabolic grain growth model accurately describes the experimental data of ZnO grain size obtained by DC magnetron sputtering technique. The fit between the model and experimental results allowed predicting grain size evolution as a function of annealing time and temperature. However, any information concerning micro-structural evolution during annealing process has not been mentioned. In fact, controlling grain size as a function of time and temperature is something worth studying. Our contribution is intended to the application of the classical nucleation and growth theory to study the effect of annealing condition (time and temperature) on grain size and film orientation. The model is based on nucleation and growth rate expressions and uses properties of the deposited material as well as the substrate such as: the melting point, the surface energy of ZnO, the interface energy and the strain energy between the substrate and the thin layer. The aim is to describe the distribution of grain size as a function of time. The thin film microstructure is modeled by a discredited three-dimensional (3D) lattice. In addition, the model of population balance equation (PBE) is widely applied for the description of the evolution of particle size for many dynamic systems such as; polymerization, precipitation, crystallization, etc. This equation can be solved by different ways including approximate methods like auxiliary methods [28] and numerical methods such as: the fixed pivot method, mobile pivot, finite difference method and finite volume method, etc. [29]. However, Monte Carlo method is a good option in the simple case of PBE equations including only the mechanism of nucleation and growth [30]. In this work, ZnO thin films have been deposited on silicon substrates using sol-gel method. The elaborated layers have been analyzed by X-ray diffraction (XRD) and atomic force microscopy (AFM) in order to correlate the structural and morphological properties with simulation results.

2. Experimental Part

Thin ZnO films were synthesized by a sol-gel method and spin-coated on silicon Si (100) substrate. The primitive solution was composed of precursor species: zinc acetate di-hydrate ($Zn(CH_3COO)_2.2H_2O$), Isopropanol (C_3H_8O) as a solvent and diethanolamine ($C_4H_{11}NO_2$) DEA as stabilizing agent. The concentration of zinc acetate was chosen to be 0.5M and the molar ratio [ZAD/DEA] equal to 1. The mixed solution was stirred with a magnetic stirrer at 60°C for 1 hour to form a transparent solution serving as the coating solution. Thin films were spin coated on silicon Si (100) substrates using KW-4A, Chemat Technology inc spin coater. The spinning speed used according to two stages was 1500/10s and 3000/20s successively. The silicon substrates are placed on the hot plate for almost 10 min to dry at 80°C. The drying procedure was repeated ten times for each film. Finally, thin films were annealed in a furnace (Nabertherm 30-3000°C) at different temperature 350°C, 400°C, 450°C and 500 °C for 1h under atmospheric conditions. The elaborated ZnO thin films were characterized by X-ray diffraction to determine crystal structure, crystal size and crystal

orientation and atomic force microscopy to evaluate grain size distribution and surface morphology.

3. Theoretical Approach

Thin films prepared by chemical deposition methods are obtained in the crystallization step by post deposition thermal annealing. This step is very important in thin films manufacturing since it not only allows the growth of the grains but it can also cause changes in their crystal orientation [31]. In the case of thin films prepared by the sol gel technique, the chemical solution deposited over the substrate, undergoes several steps such as solvent evaporation and precursor species decomposition by pyrolysis, yielding an amorphous film structure. The transformation of the structure from its amorphous to crystalline state usually takes place in the thermal annealing step. This transformation is governed through two successive mechanisms: nucleation and grain growth and thus the competition of these two mechanisms [31,32]. The nucleation and growth mechanisms start on the substrate surface before propagating into the bulk. Indeed, the theory of nucleation and growth has been widely applied as a typical approach to understand the crystallization behavior [32, 33]. The grain size in the crystallization process is governed by the Population Balance Equation given by the following general formula [30]:

$$\frac{\partial n}{\partial t}+\frac{\partial (Gn)}{\partial g}=Q_{agg}-Q_{break}-Q_{nuc} \quad (1)$$

This general equation describes the grain density number n of size g at a time t according to different phenomena such as: the growth G, aggregation Q_{agg}, breakage Q_{break} and nucleation Q_{nuc}. We assume that nucleation and growth phenomena are dominant in thin film crystallization. So, all other effects are neglected. Therefore, equation (1) will be reduced to:

$$\frac{\partial n}{\partial t}+\frac{\partial (Gn)}{\partial g}=Q_{nuc} \quad (2)$$

B, G are nucleation and growth rates, respectively.

3.1. Grain nucleation in amorphous phase

The general form of the nucleation rate is given by the following equation [34]:

$$B=J_0\left[exp\left[-\frac{\Delta G^*}{RT}\right]\right] nuclus/s.m^3 \quad (3)$$

J_0 is the nucleation rate prefactor , R is the Boltzmann constant and ΔG^* is the nucleation barrier for homogeneous or heterogeneous nucleation. The nucleation behavior of amorphous films was derived from the standard theory of crystallization in glasses. The prefactor rate J_0 is defined by [35]:

$$J_0=\upsilon N\left[exp\left[-\frac{E_a}{RT}\right]\right] \quad (4)$$

υ , is the vibrational frequency of atom, defined as the number of times per second that an atom cross the liquid-embryo, N is the number of atom per unit volume and E_a is the activation energy for atomic jump called the kinetic barrier to nucleation.

ΔG^* is the Gibbs free energy barrier given by the following formula [35] :

$$\Delta G^*=\frac{16\pi\gamma_{ac}^3 V_m^2}{3(\Delta G_v)^2}f(\theta) \quad (5)$$

ΔG_v is the change free energy calculated as follow [36]:

$$\Delta G_v=\left(\frac{\Delta H_f(T_m-T)}{T_m}\left(\frac{2T}{T_m+T}\right)\right)^2 \quad (6)$$

T , T_m and ΔH_f are growth and melting temperature and enthalpy of fusion, respectively. γ_{ca} is the interface energy between crystal and amorphous phase. It is calculated by the Turnball formula [37]:

$$\gamma_{ca}=\Phi\left(\frac{V_m}{NA}\right)^{\frac{1}{3}}\frac{\Delta H_f}{V_m} \quad J/m^2 \quad (7)$$

Φ is a constant (Φ=0.45), NA is the number of Avogadro, f(θ) is a function depending on the angle of substrate-crystal contact given by:

$$f(\theta)=\frac{(2+cos\,\theta)(1-cos\,\theta)^2}{4} \quad (8)$$

θ is the substrate-crystal contact angle

Nucleation mechanism starting at the surface of the substrate is known as heterogeneous nucleation rate (nucleus/s.m^3) is expressed as follow [38]:

$$B=\upsilon N\left[exp\left(-\frac{E_a}{RT}\right)\right]\left[exp\left[-\frac{16\pi\gamma_{ac}^3V_m^2}{3RT\left(\frac{\Delta H_f(T_m-T)}{T_m}\left(\frac{2T}{T_m+T}\right)\right)^2}f(\theta)\right]\right] \quad (9)$$

We consider a homogeneous nucleation mechanism in the bulk. In this case, nucleus is perfectly spherical. The homogeneous nucleation rate is given by:

$$B=\upsilon N\left[exp(-\frac{E_a}{RT})\right]\left[exp\left[-\frac{16\pi\gamma_{ac}^3V_m^2}{3RT\left(\frac{\Delta H_f(T_m-T)}{T_m}\left(\frac{2T}{T_m+T}\right)\right)^2}\right]\right] \quad (10)$$

After the formation of nucleus in amorphous phase, the grain growth occurs in two stages: an amorphous phase growth followed by a merging of grain boundaries between grains in the crystalline structure form.

3.2. Grain growth in amorphous phase

Based on transition state theory the growth rate (m/s) is expressed by [35]:

$$G=\frac{dg}{dt}=\lambda\upsilon\left[exp\left(\frac{-E_a}{RT}\right)\right]\left[1-exp\left[-\frac{\Delta G_g}{RT}\right]\right] \quad (11)$$

λ , ΔG_g are the jump distance and driving force for growth.

The jump distance λ defined as follows [35]:

$$\lambda=\left(\frac{V_m}{NA}\right)^{\frac{1}{3}} \quad (12)$$

For grain growth in amorphous phase, the growth rate (G) may be modified to account for surface and interfacial energy as in Eq. (3), [38,39], where λ , g, h, γ_{gb} , γ_i , γ_s ΔG_e ,ΔG_v are the jump distance, grain radius, thin film thickness, grain boundary energy,

interfacial energy, surface energy, elastic strain energy and difference in volume free energy, respectively.

The interfacial energy γ_i between substrate and amorphous thin film can be written as [40]:

$$\gamma_i = \gamma_{surface-film}^{interaction} + \gamma_{surface-film}^{enthalpy} + \gamma_{surface-film}^{entropy} \quad (14)$$

The interfacial energy between crystalline phase (nucleus) and substrate can be expressed as:

$$\gamma_i = \gamma_{surface-film}^{interaction} + \gamma_{surface-film}^{Lattice\ mismatch} \quad (15)$$

$$\gamma_{surface-film}^{lattice\ mismuch} = h\frac{E}{1-v}\varepsilon^2 \quad (16)$$

E , v and ε are the Young module, Poison ratio and lattice mismatch, respectively.

The interaction energy between substrate and film can be written as:

$$\gamma_{surface-film}^{interaction} = 0.15\left(\gamma_{substrate}^{surface} + \gamma_{film}^{surface}\right) \quad (17)$$

The enthalpy $\gamma_{surface\_film}^{enthalpy}$ can expressed as:

$$\gamma_{surface-film}^{enthalpy} = 2.19 \times 10^{-9}\left(\frac{\Delta H_f}{V_m^{\frac{2}{3}}}\right) \quad (18)$$

The entropy $\gamma_{surface\_film}^{entropy}$ is calculated as:

$$\gamma_{surface\_film}^{entropy} = \frac{S \times T_m}{V_m^{\frac{2}{3}}} \quad (19)$$

S is the surface entropy.

The strain energy term is expressed as:

$$\Delta G_e = \Delta M \times \varepsilon^2 \quad (20)$$

ΔM is the difference in the biaxial modulus of the crystalline phase and substrate or the crystalline and amorphous phases and ε is the lattice mismatch strain. It assumed that the strain energy was neglected in the amorphous-crystalline phases [40].

3.3. Grain growth in crystalline phase

According to Hillert's theory, for polycrystalline films, grain growth involves the reduction of grain boundaries, and the film becomes dense in this case the grain growth rate can be written as [41]:

$$G = \frac{dg}{dt} = M\gamma_{gb}\left(\frac{1}{\bar{g}} - \frac{1}{g}\right) \quad (21)$$

$\bar{g}$ is the average grain size.

M is the mobility of atom across the boundary given by [42]:

$$M = \frac{DV_m}{\lambda RT} \quad (22)$$

D is the diffusion coefficient which can be expressed as :

$$D = \delta\lambda^2 v\left(exp\left(-\frac{E_a}{RT}\right)\right) \quad (23)$$

Substituting Eq. (23) through Eq. (22) into Eq. (21) we obtain the grain growth rate in a polycrystalline structure as follow:

$$G = \lambda v\left[exp\left(\frac{-E_a}{RT}\right)\right]\left[\frac{\delta V_m \gamma_{gb}}{RT}\left(\frac{1}{\bar{g}} - \frac{1}{g}\right)\right] \quad (24)$$

δ is a numerical factor ($\delta = 0.1$)

The modified growth rate expression to include surface and interface energy minimization, can be written in Eq. (5) [38,39], where $\Delta\gamma_{ic} = \gamma_{i\{hkl\}} - \gamma_{i\{h\prime k\prime l\prime\}}$, $\Delta\gamma_{sc} = \gamma_{s\{hkl\}} - \gamma_{s\{h\prime k\prime l\prime\}}$ are the difference in interfacial energies between the substrate (surface) and different grain orientations in thin film.

Equation(2), satisfy the following initial condition: $n(g,0) = n_0(g)$, where $n_0(g)$ is the initial density of grains.

4. Simulation method

The three dimensional lattice of 100 x 100 x 150 grids used in the simulation process is illustrated in Fig. (1) with a uniform descritization and the distance between lattice points of d=1nm. In three dimensional simulations of thin film, the interface substrate-film presented a free surface with a normal direction parallel to the z-axis of the structure. This means that all three cubic lattices have 17 neighbors at the top of substrate, while all the other in the bulk of the lattice have 26 neighboring as mentioned by D. Zöllner [22]. Generally, in the phase characterization of ZnO thin films prepared by sol gel method the three crystallographique directions (002), (101) and (100) are more frequently illustrated [43]. The ZnO grain growth at the surface of the substrate is generally activated by the relative lower surface energy [44]. In this study, we assume that the nuclei placed on the surface (substrate-ZnO) are oriented along the (002) plane contrary to the bulk nucleation which have random orientations limited to the three directions (002), (101) and (100) and no film surface nucleation.

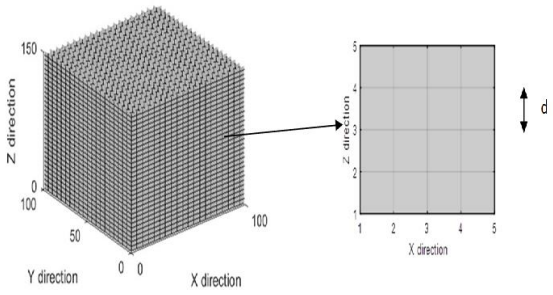

Fig. (1) The initial shape of the simulated structure

Equation (2), satisfy the following initial condition at t=0: $n(g,0) = n_0(g)$ where $n_0(g)$ is the initial density of grains. Thin film structure was presented as uniform matrix with a cell size of $n_0 = 100 \times 100 \times 150$ particles.

5. Simulation procedure

Since the problem contains only nucleation and growth in the volume, Monte Carlo method has been used for solving population balance equation. In this case, the time step which is the increment for the occurrence of nucleation or growth events is obtained from the following equation [45]:

$$\Delta t = \frac{C}{N}\frac{1}{\sum B} \quad (18)$$

N is the initial number of particles in the selected sample and C is the concentration, calculated by the

ratio between the total volume of the sample V and the average volume of the grains $\bar{v}$.

$$C = \frac{V}{\bar{v}} \quad (19)$$

Crystallization behavior is governed through two successive competitive mechanisms: nucleation and grain growth. The nucleation and growth mechanisms start on the surface of the substrate before propagating to the bulk, and then may grow according to their growth rate. The grain growth was achieved by the minimization of surface, interface and strain energies using metropolis algorithm. Assuming a constant volume as events occur, the grain number will increase or decrease over time in the simulation. As a consequence, the initial number in the sample must be restored. In our case, the number of grain in front volume was balanced with respect to surface growth in such way that the number of grain vary between N_0 and $N_0/2$. When the number of grain reaches $N_0/2$, the population is doubled back to N_0. Once the final time is reached, a logarithmic discretization rule is used to divide the size of the grains domain into a number of discrete size intervals Δg. The distribution of the grain size is presented using the grain number density function which is the solution of the population balance equation given by [46]:

$$n(g,t) = \left(\frac{n_p(l)}{n_s(l)}\right)\frac{n_{tot}}{\Delta g} \quad (20)$$

n_{tot} is the sum of grains in the grain interval (Δg)

Finally, the final film structure such as grain size, crystallinity and grain size distribution was evaluated.

6. Results and discussion

Figure (2a, b, c and d) shows XRD spectra recorded for ZnO thin films deposited on silicon substrates with various annealing temperatures (350°C, 400°C, 450°C and 500°C). XRD patterns show a preferred orientation along (002) plane corresponding to the hexagonal wurtzite structure for all ZnO thin films at different annealing temperatures. The existence of various peaks indicates that the ZnO films has polycrystalline structure. the major peaks obtained at 2θ are 31.72°, 34.6°, 36.4°, 63° correspond to the orientation (100), (002), (101) and (103) of ZnO crystals, respectively. The peaks related to (002) plane becomes most intense with increasing annealing temperature leading to the increase in the average size crystallites. It may be seen that the intensity in the (101) plane is higher than (100). This behavior was attributed to their lowest surface energy than (100) plane [47].

The crystallite size D(nm) of thin films was calculated using Debye-Scherrer formula [48]

$$D = \frac{k\lambda}{\beta.cos(\theta)} \quad (21)$$

where k is the constant value of 0.9, λ is the x-ray wavelength used in XRD instrument (0.1540nm), β is the full-width at half maximum (FWHM) of diffracting peak, and θ is the diffraction angle that defines the crystalline orientation of the ZnO thin film. Table (1) summarize information about 2θ (°) values, FWHM, grain size for different post-annealing temperature. It is noted that the FWHM value of (002) plane gradually decreases as the annealing temperature increases from 350 to 500 °C, indicating the increase in crystallite size from 17 to 21 nm . There are several explanations that may be found for the annealing effect on grain size growth. As an example, Gu et al. [49] has reported that increasing in annealing temperature leads to the diffusion process between crystallites improving grain growth. Consequently, ZnO crystallites size increase and thin film becomes more compact. Amakali [50] suggested that crystalline quality improvement with preferential orientation (002) was attributed to lowest free energy comparing with others orientation. Growth along the plane (002) is characterized by their lowest surface energy of 1.6 J/m^2 compared to the other orientations [44].

Table (1) Structural parameters of ZnO thin film obtained from XRD results

Temperature (°C)	Peak position (2θ)	FWHM (β) (002)	Crystallite size D (nm)
350	34.5818	0.63471	13.10
400	34.6546	0.62347	13.34
450	34.6260	0.51582	16.12
500	34.5621	0.47356	17.56

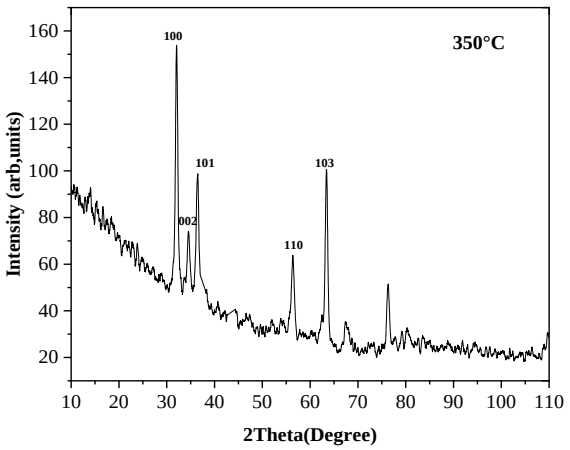

(a)

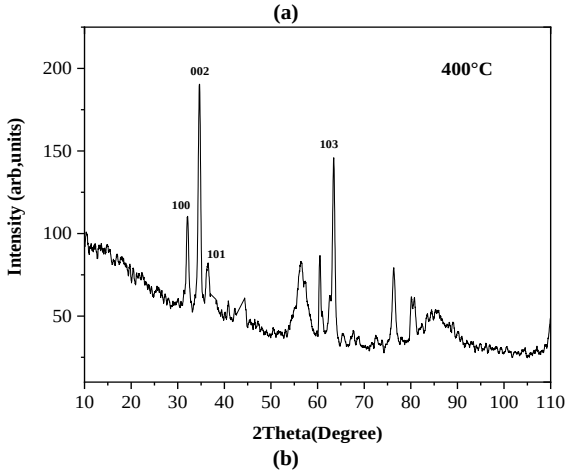

(b)

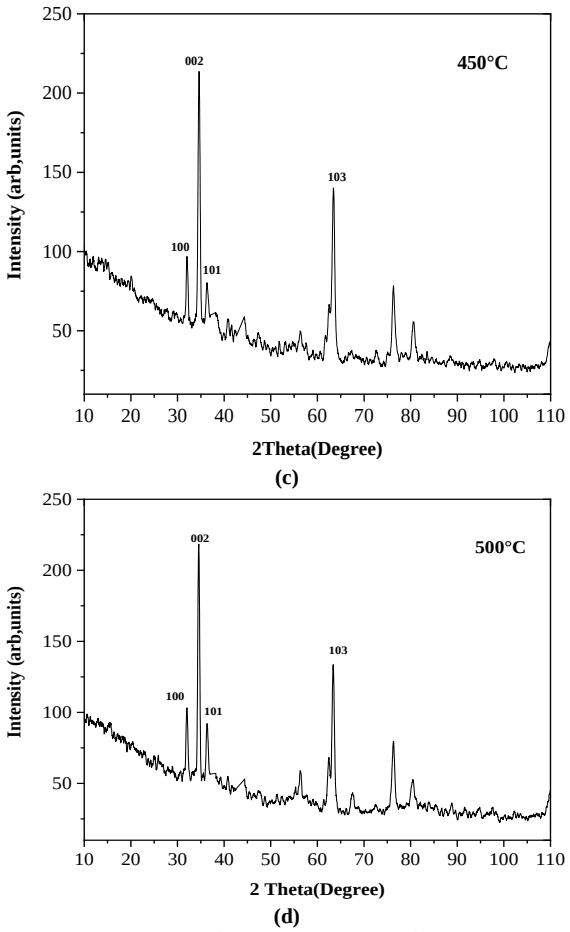

Fig. (2) XRD patterns of annealed ZnO thin films at (a) 350°C, (b) 400°C, (c) 450°C, and (d) 500°C

Figure (3) shows the 3D AFM images and grains size distribution taken at a scan of 1x1 μm^2 surface morphology of thin films annealed at 350°C, 400°C and 500°C recorded by AFM. The surface roughness mean square (RMS) of the elaborated ZnO thin films were about 1.32 nm, 4.44 nm and 5.70 nm for film annealed at 350°C, 400°C and 500°C, respectively. According to AFM images, ZnO grains are distributed uniformly over silicon substrate and appeared relatively rough. The surface roughness of ZnO thin films increases with increasing annealing temperature. Similar behavior has been observed by Rajan et al. [51]. They have reported that the surface roughness rises with increasing annealing temperature which is attributed to organic element vaporization during preheating step. Effectively, as annealing temperature increase the grains distribution at the ZnO thin film surface become not uniform by grain agglomeration. As a result, the growth of the large number of grains yields an increase in surface roughness. Moreover, the increases in grain size could be ascribed to the coalescence of small grains to form larger grains [52]. The distributions of the grain size for annealing temperatures of 350°C, 400°C and 500°C are plotted in Fig. (3).

From the obtained results, the differences between curves are clearly visible. The maximum volume fraction of the total grain was reduced from 3% to 2% with increasing annealing temperature. This variation is followed by an increase of the surface grains from 100 nm^2 to 200 nm^2 improving a grain growth during thermal annealing. Kumar et al. [24] described grain growth behavior as follow: at lower time, the formation of small grains is favored limiting the super saturation and allow grain coalescence. As the temperature or time annealing is increased the coalescence of grains will be dominate due to thermal energy.

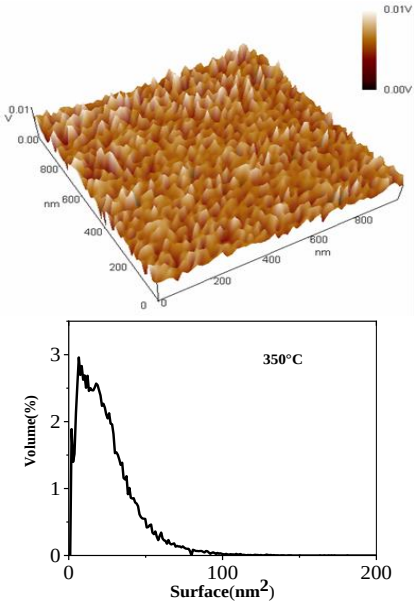

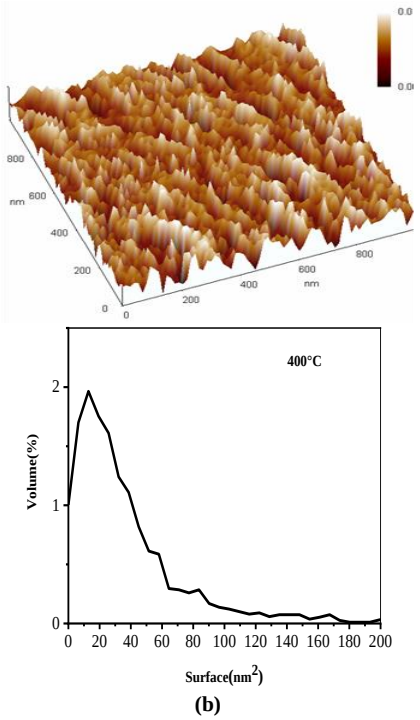

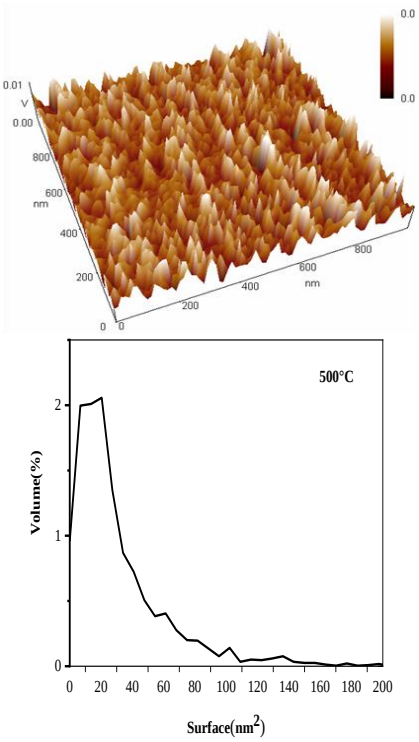

Fig. (3) 3D AFM images of ZnO films annealed at temperature of (a) 350°C, (b) 400°C, and (c) 500°C

According to the above formulation, we investigate the effect of temperature and annealing time on grain size and crystalline quality of ZnO thin films in a three-dimensional structure. Then, we analyze the grain size distribution law to show growth behavior. The average grain size evolution as a function of annealing temperature 350°C, 400°C, 450°C and 500°C for fixed annealing time of 60 min are shown in Fig. (4) for the three crystallographic orientation (100), (101) and (002). From Fig. (4), it can be noticed that the average grain size of the more pronounced orientation (002) increase from 20 to 24 nm with increasing annealing temperature. With the increase of annealing temperature the crystallinity percentage increases to 46.59% ensuring a growth with high-quality ZnO thin films as shown in Fig. (5). These results are in good agreement with those reported by H. Sharma et al. [53]. The grain size distribution in ZnO thin film is very important because the average size is a single propriety that doesn't give any information on how much the bigger grains dominate in the microstructure.

Figure (6) illustrates the grain size distribution of ZnO films annealed at various temperatures calculated in previous section. From Fig. (6), the values of the grain size distribution seems to follow a Gaussian law, then this distribution decreases continuously to larger sizes grains with a displacement of the distribution band towards larger sizes. The decrease in the value of grain number can be attributed to the increase in growth rate; consequently the grains increase in size in favor of smaller grains. In order to compare, our simulation and experimental results we have chosen the preferred crystal growth in (002) plane.

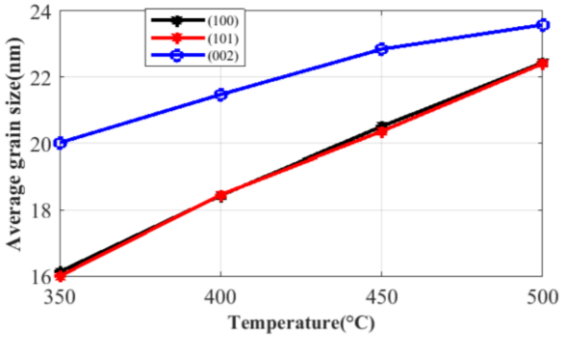

Fig. (4) Variation of average grain size as a function of annealing temperatures for different orientations

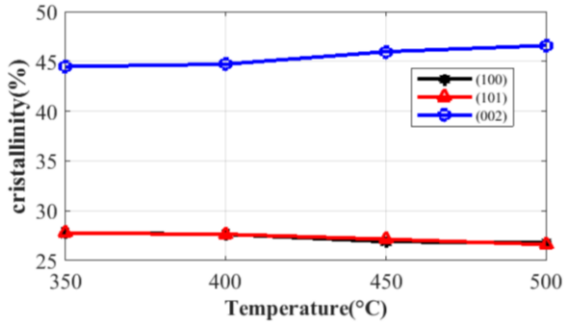

Fig. (5) Variation of percentage crystallinity as a function of annealing temperatures for different orientations

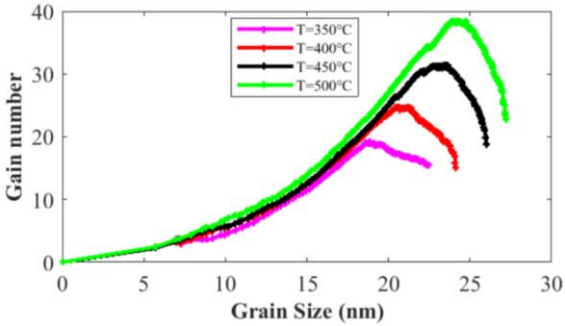

Fig. (6) Grain size distribution at different temperatures: 350°C, 400°C, 450°C and 500°C

From Fig. (7), the simulation results roughly approached to experimental data. Figure (8) shows the simulated microstructures for annealing temperatures of 350 °C and 500°C. The simulation results for 350°C show that overall grain size are randomly oriented and no considerable grain growth is observed until the annealing temperature reached 500°C, as shown in Fig. (8b).

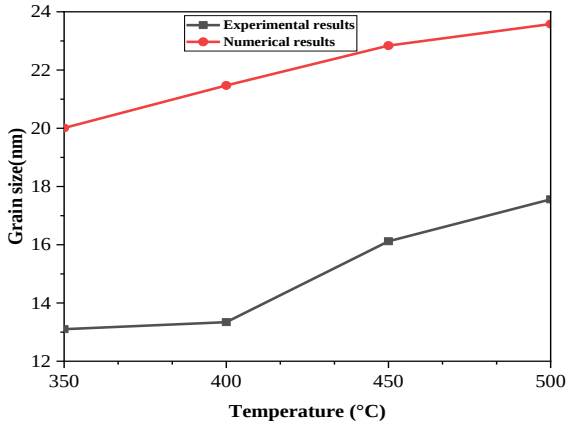

Fig. (7) Comparison between experimental and simulation results of the grain size in (002) orientation

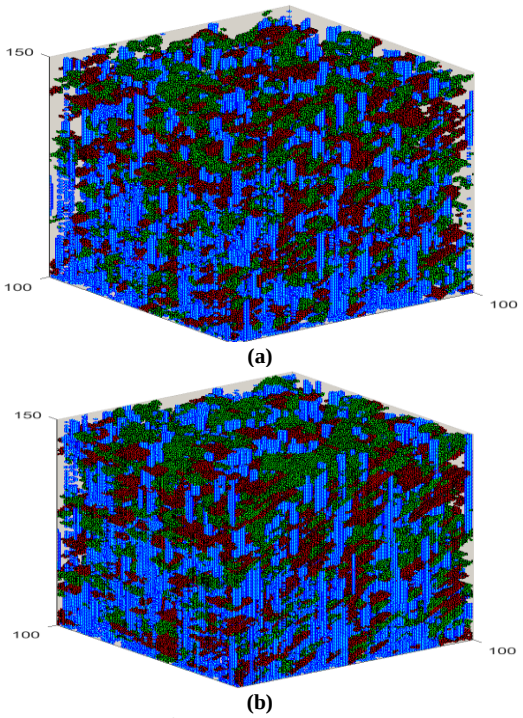

Fig. (8) 3D evolution of grain structure at annealing temperature of (a) 350°C and (b) 500°C for the three orientations: Red (100), Green (101), Blue (002)

7. Conclusion

This study was focused on grain growth in sol gel ZnO thin films during crystallization in annealing step. Theoretical approach based on population balance equation (PBE) has been formulated for the description of the grain size distribution during the crystallization step as a function of post deposition annealing conditions. The theoretical model was developed for thin ZnO films synthesized by the sol-gel method on silicon substrates with a thickness of about 150 nm. This study has investigated the annealing optimization process of ZnO films by adopting the optimal parameters to obtain good thin film quality using the Monte Carlo (MC) simulation method. The relationship between the changes in surface roughness and volume fraction of the ZnO grain has been analyzed. From AFM topography, increasing annealing temperature leads to the grain size increase. The simulation results show that the grain size distribution follows a Gaussian law as a function of temperature and the crystallite size increase with annealing temperature.

References

[1] X. Li et al., "Study on structural and optical properties of Mn-doped ZnO thin films by sol-gel method", *Opt. Mater.*, 100 (2020) 109657.

[2] I. Ameur et al., "Influence of magnesium doping on microstructure, optical and photocatalytic activity of zinc oxide thin films synthesis by sol–gel route", *Appl. Phys. A.*, 127 (2021) 1007.

[3] R. Ebrahimifard, H. Abdizadeh and M. R. Golobostanfard, "Controlling the extremely preferred orientation texturing of sol–gel derived ZnO thin films with sol and heat treatment parameters", *J. Sol-Gel Sci. Technol.*, 93 (2020) 28–35.

[4] C.N. Wang et al., "Advances in Doped ZnO Nanostructures for Gas Sensor", *Chem. Rec.*, 20 (2020) 1–16.

[5] F. Dabir et al., "Study on microstructural and electro-optical properties of sol–gel derived pure and Al/Cu-doped ZnO thin films", *J. Sol-Gel Sci. Technol.*, 96(3) (2020) 529–538.

[6] A.K. Ambedkar et al., "Structural, optical and thermoelectric properties of Al-doped ZnO thin films prepared by spray pyrolysis", *Surf. Interfaces*, 19 (2020) 100504.

[7] M. Lakhdari and F. Habelhames, "Morphological and structural control of pulse electrodeposited ZnO thin films and its influence on the photoelectrocatalytic degradation of methyl orange", *J. Mater. Sci. Mater. Electron.*, 30(6) (2019) 6107–6115.

[8] M.R. Islam et al., "Structural, optical and photocatalysis properties of sol–gel deposited Al-doped ZnO thin films", *Surf. Interfaces*, 16 (2019) 120–126.

[9] S. Benramache et al., "Effect of annealing temperature on structural, optical and electrical properties of ZnO thin films prepared by sol-gel method", *J. Nano Electron. Phys.*, 10 (6) (2018) 06032.

[10] N. Ben Moussa et al., "Synthesis of ZnO sol-gel thin-films CMOS-Compatible", *RSC Adv.*, 11(37) (2021) 22723–22733.

[11] D.T. Speaks, "Effect of concentration, aging, and annealing on sol gel ZnO and Al-doped ZnO thin films", *Int. J. Mech. Mater. Eng*., 15(2) (2020) 1186.

[12] J. Li, D. Yang and X. Zhu, "Effects of aging time and annealing temperature on structural and optical properties of sol-gel ZnO thin films", *AIP Adv*., 7(6) (2017) 065213.

[13] N. Kasim et al., "Morphological and structural properties of Sol-Gel derived ZnO thin films spin-coated on different substrates", *Solid State Phenom.*, 301 (2020) 35–42.

[14] A.B. Khatibani, "Investigation of gas sensing property of zinc oxide thin films deposited by Sol-Gel method: effects of molarity and annealing temperature", *Indian J. Phys.*, 95(2) (2021) 243–252.
[15] N. Motlan, N. Siregar and J. Panggabean, "The effect of post annealing time on structural and optical properties of ZnO thin films by sol-gel spin coating method", *J. Phys. Conf. Ser.*, 1428 (2020) 012065.
[16] M. Arif et al., "Effect of Annealing Temperature on Structural and Optical Properties of Sol–Gel-Derived ZnO Thin Films", *J. Electron. Mater.*, 47(7) (2018) 3678–3684.
[17] B. Sharmila, M.K. Singha and P. Dwivedi, "Impact of annealing on structural and optical properties of ZnO thin films", *Microelectron. J.*, 135 (2023) 105759.
[18] L. Arab et al., "Effect of the annealing process on the properties of ZnO thin films prepared by the sol-gel method", *Chem. Phys. Impact.*, 7 (2023) 100266.
[19] D.B. Mitzi, **"Solution processing of inorganic materials"**, John Wiley & Sons, Inc. (2009), Ch. 2, pp. 53-65.
[20] D. Zöllner and W. Pantleon, "Grain growth in thin film under strong temperature gradients", *IOP Conf. Series: Mater. Sci. Eng.*, 1249 (2022) 012010.
[21] E. Miyoshi et al., "Large-scale phase-field simulation of three dimensional isotropic grain growth in polycrystalline thin films", *Model. Simul. Mater. Sci. Eng.*, 27 (2019) 054003.
[22] D. Zöllner, "Treating grain growth in thin films in three dimensions: A simulation Study", *Comput. Mater. Sci.*, 125 (2016) 51–60.
[23] Z.J. Luan et al., "Effect of interface energy on abnormal grain growth in pyrite films prepared by sol–gel method", *Mater. Res. Bull.*, 46 (2011) 1577–1581.
[24] V. Kumar et al., "Effect of annealing on the structural, morphological and photoluminescence properties of ZnO thin films prepared by spin coating", *J. Colloid Interface Sci.*, 428 (2014) 8-15.
[25] A.A. Joraid et al., "Studies of crystallization kinetics and optical properties of ZnO films prepared by sol–gel technique", *J. Sol-Gel Sci. Technol.*, 97 (2021) 523–539.
[26] N. Bouhssira et al., "Isothermal crystallization kinetic of ZnO thin films", *J. Cryst. Growth*, 312 (2010) 3282–3286.
[27] O.A. Hammadi, "Preparation of ZnO thin films using DC sputtering method", *Iraqi J. Phys.*, 2(3) (2003) 1-6.
[28] Z. Pınar et al., "Analytical Solution of Population Balance Equation Involving Growth, Nucleation and Aggregation in Terms of Auxiliary Equation Method", *Appl. Math. Inf. Sci.*, 9(5) (2015) 2467-2475.
[29] A. Majumder et al., "Lattice Boltzmann method for population balance equations with simultaneous growth, nucleation, aggregation and breakage", *Chem. Eng. Sci.*, 69 (2012) 316–328.
[30] C.F. Lu and L.A. Spielman, "Kinetics of floc breakage and aggregation in agitated liquid suspensions", *J. Colloid Int. Sci*., 103 (1985) 95-105.
[31] K.S. Lokesh et al., "Experimental evaluation of substrate and annealing conditions on ZnO thin films prepared by sol-gel method", *Mater. Today Proc.*, 24 (2020) 201–208.
[32] S. Fujihara, C. Sasaki and T. Kimura, "Crystallization behavior and origin of c-axis orientation in sol-gel-derived ZnO:Li thin films on glass substrates", *Appl. Surf. Sci.*, 180 (2001) 341–350.
[33] M.H. Nateq and R. Ceccato, "Enhanced Sol-Gel Route to Obtain a Highly Transparent and Conductive Aluminum-Doped Zinc", *Materials*, 12 (2019) 1744.
[34] M. Muthukumar, **"Nucleation in polymer crystallization"**, in Advances in Chemical Physics, vol. 128, S.A. Rice (ed.), John Wiley & Sons, Inc. (2004), p. 25.
[35] M.W. Barsoum, **"Series in Materials Science and Engineering Fundamentals of Ceramics"**, Department of Materials Engineering, Drexel University, USA (2003), pp. 265-275.
[36] C.V. Thompson and F. Spaepen, "On the approximation of the free energy change on crystallization", *Acta Metallurg.*, 27 (1979) 1855-1859.
[37] S.K. Pillai et al., "Nucleation and growth in amorphous $(GeS_2)_{0.9}(Sb_2S_3)_{0.1}$ thin films", *J. Cryst. Growth*, 382 (2013) 87–93.
[38] L. Challat and A. Bellel, "Modeling of grain size growth in pure ZnO thin films prepared by the sol gel method", *2nd Int. Conf. Adv. Electr. Eng. ICAEE 2022, IEEE* (2022).
[39] H. Dobberstein and R.W. Schwartz, "Modeling the Nucleation and Growth Behavior of Solution Derived Thin Films", *Proc. 1st Symp. Adv. Mater. for Next Gen. Prelude to Func. Integr. Mater.*, AIST Chubu, Nagoya, Japan May 27, 2002.
[40] L.P.H. Jeurgens et al., "Thermodynamic stability of amorphous oxide films on metals: Application to aluminum oxide films on aluminum substrates", *Phys. Rev. B*, 62 (2000) 4707-4719.
[41] C.V. Thompson et al., "Epitaxial grain growth in thin metal films", *J. Appl. Phys.*, 673 (1990) 4099.
[42] Y.M. Chiang et al., **"Physical Ceramics"**, John Wiley & Sons, Inc. (NY, 1997), pp. 351-513.
[43] A. Rajan, V. Gupta and K. Arora, "Thickness dependent ultraviolet photoconductivity studies on sol-gel derived zinc oxide (ZnO) films", *Mater. Today Commun.*, 35 (2023) 105507.
[44] X.L. Chen et al., "Temperature-dependent growth of zinc oxide thin films grown by metal organic chemical vapor deposition", *J. Cryst. Growth*, 296 (2006) 43–50.
[45] H. Zhao et al., "Analysis of four Monte Carlo methods for the solution of population balances in dispersed systems", *Powder Technol*., 173 (2007) 38–50.

[46] D. Meimaroglou, A.I. Roussos and C. Kiparissides, "Part IV: Dynamic evolution of the particle size distribution in particulate processes. A comparative study between Monte Carlo and the generalized method of moments", *Chem. Eng. Sci.*, 61 (2006) 5620 -5635.
[47] M. Rouchdi et al., "Synthesis and characteristics of Mg doped ZnO thin films: Experimental and ab-initio study", *Results. Phys.*, 7 (2017) 620–627.
[48] W.C. Lim et al, "Effect of thermal annealing on the properties of ZnO thin films", *Vacuum*, 183 (2021) 109776.
[49] P. Gu, X. Zhu and D. Yang, "Effect of annealing temperature on the performance of photoconductive ultraviolet detectors based on ZnO thin films", *Appl. Phys. A*: *Mater. Sci. Process*., 125(1) (2019) 50.
[50] T. Amakali et al., "Structural and Optical Properties of ZnO Thin Films Sol-Gel Methods", *Crystals*, 10(2) (2020) 132.
[51] C. Rajan, N. Pasupathy and J. Gopinath, "Crystallization and surface Morphology following annealing using ZnO thin film", *J. Adv. Schol. Res. Allied Educ.*, 19(4) (2020) 214-218.
[52] M. Sypniewska et al., "Structural, morphological and photoluminescent properties of annealed ZnO thin layers obtained by the rapid sol-gel spin-coating method", *Opto-Electron. Rev*., 28 (2020) 182-190.
[53] H. Sharma et al., "Temperature treatment effect on the physical and optical properties of ZnO thin films", *J. Mater. Sci.: Mater. Electron.*, 35(20) (2024) 1-8.

$$G = \frac{dg}{dt} = \lambda v \left[exp\left(\frac{-E_a}{RT}\right)\right]\left[\left(1 - exp\left[-\frac{\Delta G_e + \Delta G_v + \frac{\Delta\gamma_i + \Delta\gamma_s}{h} + \frac{\gamma_{ca}}{g}}{RT}\right]\right)\right] m/s \quad (13)$$

$$G = \lambda v \left[exp\left(\frac{-E_a}{RT}\right)\right]\left[\frac{\delta V_m \gamma_{gb}}{RT}\left(\frac{1}{\bar{g}} - \frac{1}{g}\right) + \left(1 - exp\left[-\frac{-\Delta G_e + \frac{\Delta\gamma_{ic} + \Delta\gamma_s}{h} + \frac{\gamma_{sc}}{g}}{RT}\right]\right)\right] m/s \quad (25)$$

